Progress In Electromagnetics Research B, Vol. 51, 177–199, 2013

DESIGN OF SLOTTED GROUND HEXAGONAL MICROSTRIP PATCH ANTENNA AND GAIN IMPROVEMENT WITH FSS SCREEN

Nagendra Kushwaha* **and Raj Kumar**

Research Scholar, Department of Electronics Engg., DIAT, Deemed University, Girinagar, Pune-411 025, A.R.D.E. Pashan, Pune-411 021, India

Abstract—Three hexagonal patch antennas are designed for circular polarization and experimentally validated. These antennas are labeled; simple hexagonal patch, hexagonal patch with slotted ground and hexagonal patch with parasitic element. The measured impedance bandwidths of the three antennas are 2% for the simple patch, 5.2% for the patch with slotted ground and 6.35% for the antenna with parasitic element. The axial ratio (measured) obtained is 4.73% for the patch with slotted ground and 3.33% for the hexagonal patch antenna with parasitic element. The measured radiation patterns of these antennas are found to be in good agreement with the simulated radiation patterns. The average gain of all the three antennas is also evaluated. A frequency selective surface (FSS) is proposed with dimensions smaller than that of a conventional FSS structure. The measured gain improvement with the proposed FSS is around 3 dB in the operating band.

1. INTRODUCTION

Nowadays, circular polarization has gained much attention due to the large number of applications in wireless communication, military sensor systems and global navigation satellite systems. This is due to the fact that a circularly polarized antenna does not require alignment of electric field vector at the receiving and transmitting ends. A single patch antenna can be made to radiate circularly polarized field if two orthogonal patch modes are simultaneously excited with equal amplitude and with ± 90 degree phase difference with the sign

Received 16 March 2013, Accepted 22 April 2013, Scheduled 27 April 2013

* Corresponding author: Nagendra Kushwaha (nagendra.gcet@gmail.com).

determining the sense of rotation. This can be achieved either with two orthogonal feeds or with single feed and modified geometry. However, the problem with two feeds is that the antenna becomes bulky and requires power supplies or a power divider which increases the complexity of the circuit. On the contrary, single feed allows for reduction in size, weight, complexity and RF power loss. The common shapes used with single feed are modified versions of regular geometries like triangle, circle and square [1–7]. In addition, the performance of a patch antenna can be altered by introducing a parasitic element. The parasitic element can either be placed in the plane of the patch antenna on the same substrate or placed above it in a stacked arrangement. When the parasitic element is placed adjacent to the driven element, it increases the size of the antenna and hence it is preferably placed vertically over the feed driven patch so as to be suitable for wireless communication system.

Electromagnetic Band Gap (EBG) structures and Frequency Selective Surfaces (FSS) can be used to alter the propagation of electromagnetic waves giving many advantages including enhancement in the gain. FSS, in contrast to the EBG has low profile and hence is a better candidate for the gain enhancement of antenna [8]. FSS can also be used to improve the bandwidth [9–11]. In addition, FSS superstrate is also used as a polarizer to get circular polarization in case of single source excitation [12, 13]. It can also be used as radar absorbing material [14] and to decrease Specific Absorption Rate (SAR) [15, 16]. It can also work as a dual polarized band stop spatial filter [17].

In this paper, a simple hexagonal patch antenna has been studied and compared with the slotted ground hexagonal patch antenna and hexagonal patch antenna with parasitic element. The hexagonal patch antenna is chosen as it is capable of generating circular polarization and can be designed by using variation of static energy below a circular patch [18]. A frequency selective surface (FSS) is proposed with dimensions smaller than that of a conventional FSS structure. Further, a comparison of the performance of the proposed FSS with a conventional FSS is done in terms of their effect on return loss, bandwidth and gain. The simulated and measured results are in good agreement.

2. HEXAGONAL PATCH ANTENNA DESIGN

For designing the hexagonal patch antenna, first circular patch antenna design must be introduced because these two antennas are closely related to each other. The fundamental resonance frequency of a

circular patch antenna is given by

$$f_r = \frac{X_{mn}}{2\pi a_e \sqrt{\varepsilon_r}} c \tag{1}$$

where f_r is the resonant frequency of the patch, $X_{mn} = 1.8411$ for the dominant mode TM_{11}, c is the velocity of light in free space, ε_r is the relative permittivity of the substrate and a_e is the effective radius of the circular patch and given by

$$a_e = a\left\{1 - \frac{2h}{\pi a \varepsilon_r}\left(\ln\frac{\pi a}{2h} + 1.7726\right)\right\}^{0.5} \tag{2}$$

In the above expression, 'a' is the actual radius of the circular patch antenna as shown in Figure 1, whereas h is the height of the substrate.

The Equation (1) can be applied for designing a hexagonal microstrip patch antenna by relating the areas of the circular and hexagonal patches as shown in Equation (3).

$$\pi a_e^2 = \frac{3\sqrt{3}}{2} s^2 \tag{3}$$

where s is the side length of the hexagonal patch.

3. CONFIGURATION OF THE THREE ANTENNAS

3.1. Simple Hexagonal Microstrip Patch (HMP)

A simple hexagonal microstrip patch antenna is designed on a FR-4 substrate having dielectric constant $\varepsilon_r = 4.3$, thickness $h = 1.53$ mm and size of 50 mm × 50 mm. The side length 's' of the hexagonal patch antenna has been calculated using Equations (1)–(3) and it is found to be 11.0 mm for the central frequency $f_o = 3.5$ GHz. The simple hexagonal patch and the equivalent circle are as shown in Figure 1. For obtaining circular polarization, the feed location is placed at an optimal location from the center of the patch and at an angle of 45° from the axis.

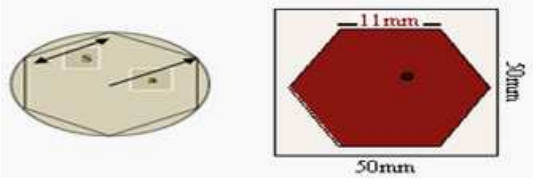

Figure 1. Simple hexagonal microstrip patch.

3.2. Hexagonal Patch with Slot in the Ground

A single triangular slot is cut in the ground plane. The antenna has been designed for the centre frequency of 3.84 GHz. This antenna is optimized by adjusting the feed position and size of the triangular slot in the ground to have the optimum impedance matching and optimum bandwidth. For this centre frequency, the optimum value of the triangular slot area (in the ground plane) and side length of the driven patch are found to be 30.75 mm^2 and 11.0 mm, respectively. The antenna has been fabricated for validating the results. The top and bottom view of the antenna are shown in Figure 2, while the side view is shown in Figure 4(a).

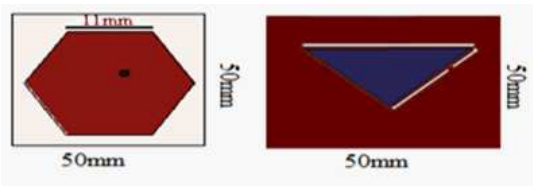

Figure 2. Hexagonal Microstrip Patch (HMP) with slot in the ground antenna.

3.3. Antenna with Parasitic Element

The slotted ground HMP with a parasitic element has also been designed. This antenna has been designed for the centre frequency of 3.55 GHz. The side length of the driven patch and the parasitic element are optimized to 11.0 mm and 10.0 mm respectively while the triangular slot area (in the ground) is optimized to 30.75 mm^2. The optimization is done by adjusting the feed position, side length of the parasitic element and size of the triangular slot in the ground plane for obtaining optimum bandwidth and return loss. The antenna has

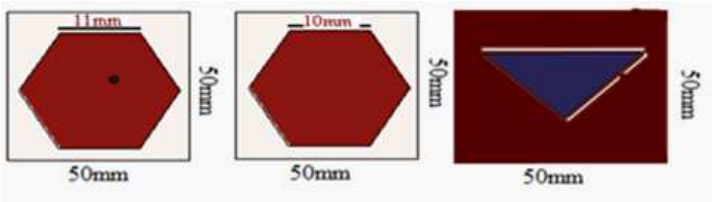

Figure 3. HMP slotted ground with parasitic element.

been fabricated to validate the simulated results. The top view and the bottom view of this antenna are shown in the Figure 3. The side view of this antenna is shown in Figure 4(b). The optimized dimensions of all the three antennas are given in Table 1.

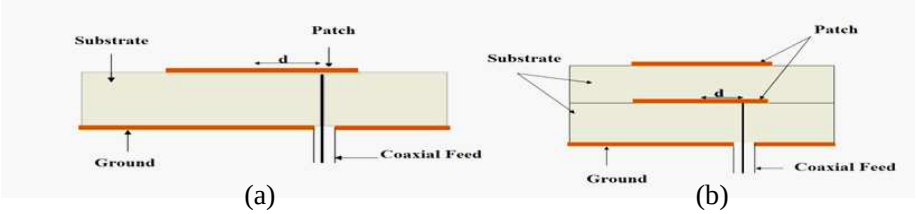

Figure 4. (a) Side view of HMP with slot in the ground. (b) Side view of HMP with parasitic element.

Table 1. Dimensions of the proposed antennas.

S. No.	Parameters (mm)	Simple HMP	HMP with Slot in Ground	HMP with Slotted Ground and Parasitic Element
1	Side Length of driven element	11.0 mm	11.0 mm	11.0 mm
2	Feed position from the centre (along diagonal)	2.96 mm	4.19 mm	4.75 mm
3	Slot surface area	-	30.66 mm^2	30.75 mm^2
4	Side length of parasitic element	-	-	10.0 mm

4. RESULTS AND DISCUSSION

4.1. Reflection Coefficient

The three antennas (Simple hexagonal patch, hexagonal patch with slotted ground and hexagonal patch stacked with parasitic patch) are designed and simulated using Ansoft HFSS and CST Microwave Studio. The antennas are then fabricated with optimized dimensions. The measurements for the fabricated prototypes were taken on a Rohde & Schwarz Vector Network Analyzer (ZVA-40). The simple

HMP is designed for the frequency of 3.5 GHz and the optimized feed location is found to be $d = 2.96$ mm from the center of the patch and along the diagonal. The measured impedance bandwidth obtained is 70 MHz from 3.45 GHz to 3.52 GHz (2% at the resonance frequency of 3.5 GHz). Then for the second antenna, a single triangular slot is cut in the ground plane and its size and feed location are optimized. The photograph of the fabricated antenna is shown in the Figure 5(a). The measured impedance bandwidth for this antenna is 200 MHz from 3.74 GHz to 3.94 GHz (5.2% at the resonance frequency of 3.84 GHz). This bandwidth is 3.2% more in comparison to the simple hexagonal patch. The measured and simulated results for this antenna are shown in Figure 5(b). The third antenna is designed by stacking another similar hexagonal patch on top of the hexagonal patch antenna with slot in the ground plane and the feed location is optimized. The photograph of the fabricated antenna is shown in Figure 6(a) while the reflection coefficient (measured and simulated) is shown in Figure 6(b). The measured impedance bandwidth obtained in this case is 230 MHz from 3.54 GHz to 3.77 GHz (6.35% at the resonance frequency of 3.6 GHz). This is 4.35% more in comparison to the simple patch and 1.15% more in comparison to the slotted hexagonal patch.

It can be seen from Figure 5(b) and Figure 6(b) that the measured and simulated reflection coefficients are in good agreement. The slight difference between the simulated results of HFSS and CST Microwave studio is due to the different numerical techniques employed by the two software. The slight difference between the measured and simulated results is due to fabrication constraints, uncertainties in the dielectric constant and the substrate thickness, soldering effects and the low quality of the SMA connector used.

The optimized feed location for the three antennas, their resonance

(a) (b)

Figure 5. (a) Photograph of HMP with slot in ground. (b) Measured and simulated return loss of HMP with slot in ground.

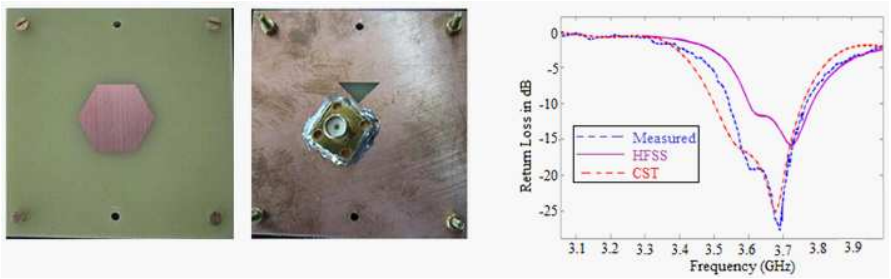

Figure 6. (a) Photograph of HMP with slotted ground and parasitic element. (b) Measured and simulated return loss of HMP with slotted ground and parasitic element.

Table 2. Resonant frequencies, impedance bandwidths and simulated gains of the three antennas.

S. No.	Antenna	Feed location (Distance from the centre along the diagonal) d (mm)	Measured Impedance Bandwidth (MHz)	Average Gain (dB)	Resonance Frequency f_o (GHz)
1	Simple HMP	2.96	70.0	6.0	3.50
2	HMP with slotted ground	4.18	200.5	6.5	3.84
3	HMP with parasitic element	4.75	221.7	6.6	3.60

frequencies, impedance bandwidths and simulated gains are given in Table 2. It can be noticed that the impedance bandwidth increases and the central frequency shifts towards the higher frequency side for both the slotted and stacked antenna against the simple patch antenna. It is also observed that the central frequency of stacked antenna shifts towards the lower frequency side as against the slotted ground antenna.

4.2. Radiation Patterns

The radiation patterns of the hexagonal patch antenna with slot in the ground plane are simulated at 3.84 GHz in the E and H planes using HFSS and CST Microwave Studio and measured in the in-house

anechoic chamber using antenna measurement system. A standard double ridged horn antenna is used as a reference antenna. The simulated and measured radiation patterns are as shown in Figure 7(a). The simulated and measured results are in close agreement. Similarly, the radiation patterns in the E and H plane of the hexagonal patch antenna stacked with a parasitic patch are simulated at 3.54 GHz and a comparison with the measured results is shown in Figure 7(b). For both the cases, the simulated and measured results are found to be in close agreement with a little difference due to measurement and alignment errors.

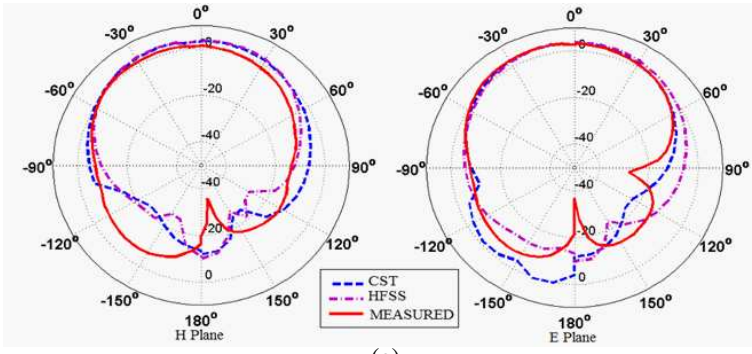

(a)

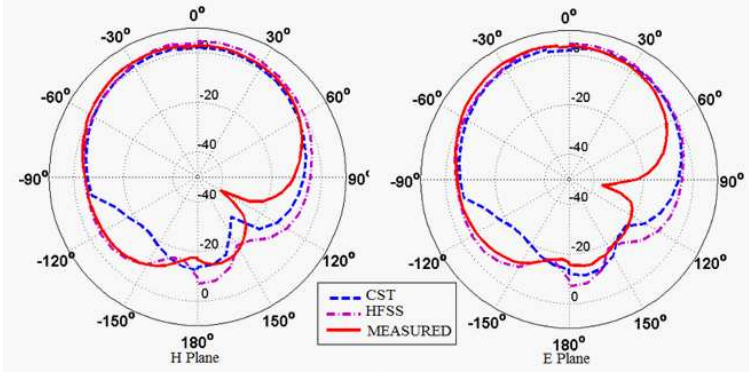

(b)

Figure 7. (a) Measured and simulated radiation patterns of hexagonal patch with slot in the ground at $f = 3.84$ GHz. (b) Measured and simulated radiation patterns of antenna with parasitic element at $f = 3.55$ GHz.

4.3. Measured and Simulated Axial Ratio

The purity of circular polarization is characterized by axial ratio. If the axial ratio is less than 3 dB over any frequency band, then the antennas are said to be circularly polarized in that frequency band. The simulated and measured axial ratios of the hexagonal patch with slot in the ground and for the antenna with parasitic element are shown in Figure 8. The simulated and measured values are in good agreement. It is observed from the figure that for the hexagonal patch with slot in the ground, the measured axial ratio bandwidth achieved is 180 MHz from 3.74 GHz to 3.92 GHz (4.7% at the center frequency of 3.83 GHz). For antenna with parasitic element, the axial ratio achieved is 120 MHz from 3.55 GHz to 3.67 GHz (3.33% at center frequency of 3.6 GHz). Therefore, it can be concluded that the axial ratio bandwidth is more in case of the patch with slotted ground in comparison to the antenna with parasitic element. The measured axial ratio bandwidth is seen to be slightly better than the simulated axial ratio bandwidth and this may be due to the characteristics of the reference horn antenna employed in the measurement system. However, the axial ratio bandwidth remains less than the impedance bandwidth as usually happens.

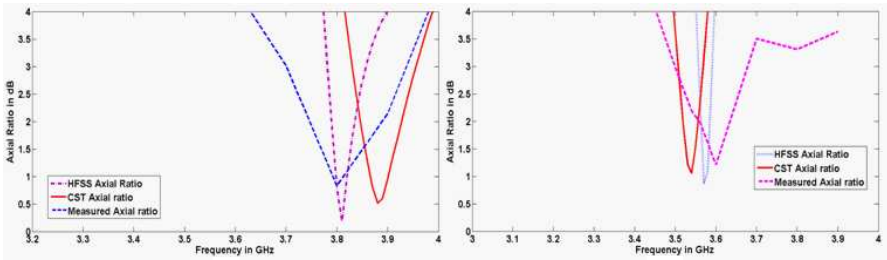

Figure 8. Simulated and measured axial ratio (dB) of (a) hexagonal patch with slot in the ground, (b) antenna with parasitic element.

4.4. Parametric Study

The dimensions of the slot in the ground plane are varied and the effect of this variation on the bandwidth and return loss of the hexagonal patch antenna with slot in the ground is studied. The area of the slot is assigned four different values. The effect of the variation in the slot area is seen from the simulated return loss curves shown in Figure 9. It can be said that, as the slot size varies, the impedance bandwidth, return loss as well as the axial ratio of the antenna varies.

It means, for having optimum impedance bandwidth and axial ratio, the slot size has to be optimized. For a slot area of 30 mm^2, the first resonance is not much pronounced and that may effect the axial ratio of the antenna. So the optimized value of the slot area is taken as 30.25 mm^2. The first and the second resonance frequencies and the simulated impedance bandwidths for the different slot areas are given in Table 3.

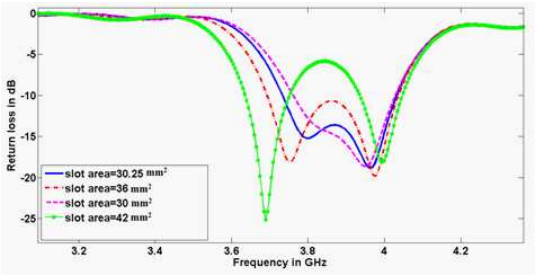

Figure 9. Simulated results of different slot size for hexagonal patch with slot in the ground.

Table 3. The effect of slot size on the impedance bandwidth for hexagonal patch with slot in the ground.

Slot Area (mm square)	1st Resonance Frequency (GHz)	2nd Resonance Frequency (GHz)	Bandwidth (MHz)
30.25	3.80	3.96	290
36	3.75	3.964	330
30	3.82	3.96	260
42.156	3.70	3.98	-

4.5. Circular Polarization

The simulated vector current distribution of the hexagonal patch with slot in the ground is shown in Figure 10 at the frequency of 3.84 GHz. As seen from the figure, the direction of the current vector changes as the phase angle of the current drawn by the antenna increases. The current vector is seen to rotate in a circular fashion with an increase of phase angle and this shows that the antenna is circularly polarized.

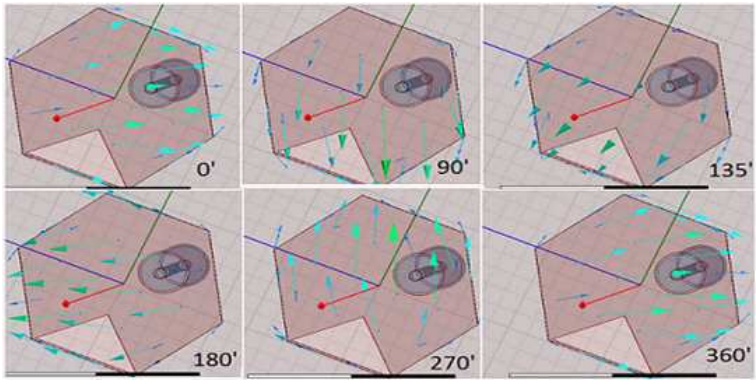

Figure 10. Simulated current vector vs phase angle at frequency $f = 3.8$ GHz for hexagonal patch with slot in the ground.

5. FREQUENCY SELECTIVE SURFACE (FSS) DESIGN

5.1. Aperture Type FSS

The simple patch antenna is normally a low gain antenna and the gain improvement is a matter of great concern for various applications. The Electromagnetic Band Gap (EBG) and the Frequency Selective Surface (FSS) are two advanced techniques available to enhance the gain. The Frequency Selective Surface is an alternative to the EBG but has a lower profile. Hence, it is a better candidate for gain enhancement [8]. An aperture type FSS having dimensions of unit patch 18 mm × 18 mm is designed and gap between each element is

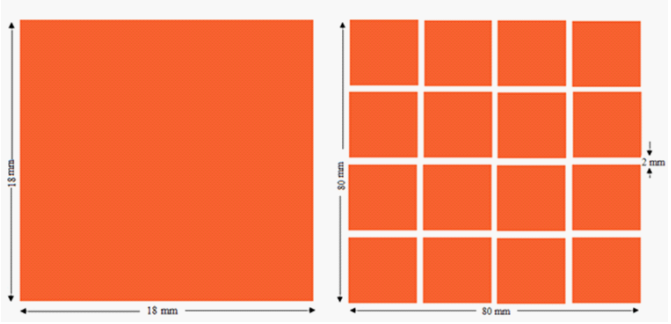

Figure 11. Aperture type FSS. (a) Unit cell. (b) 4 × 4 FSS.

taken to be 2 mm. The structure of this aperture FSS is shown in Figure 11 and the transmission characteristic is shown in Figure 12. This type of FSS shows a highly inductive nature and less capacitive nature. To have a resonance at a particular frequency, the size of aperture type FSS is more compared to the proposed FSS discussed in the following section.

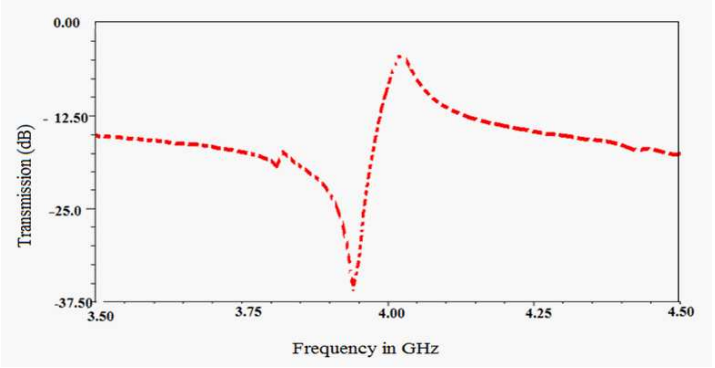

Figure 12. Simulated transmission coefficient (in dB) of aperture type FSS screen.

5.2. Proposed Frequency Selective Surface (FSS)

To overcome the disadvantage of the aperture type FSS, a new FSS is introduced, that shows a size reduction for the unit element and a better transmission response as compared to aperture type FSS. By cutting multiple slots in the patch, a capacitive effect is created and this effect gives resonance at a lower frequency as compared to the aperture type FSS of the same size. The unit size of the proposed FSS is 14 mm × 14 mm. Four slots are cut in the patch; three vertical having dimensions 2 mm × 13 mm, 2 mm × 12.5 mm and 2 mm × 12.5 mm and one horizontal slot having dimensions 13 mm × 2 mm. The gap between each unit element is taken to be 1.0 mm. The FSS structure and its response are shown in Figure 13 and Figure 15 respectively while a photograph of the fabricated 4 × 4 FSS screen is shown in Figure 14. The transmission characteristic of the proposed FSS screen is measured by placing it in the far field region between two standard horn antennas. The measured and simulated transmission coefficients are found to be in good agreement. The effect of varying the gap between the unit cells (unit cell spacing) on the transmission characteristic is shown in Figure 16. It is seen that reducing the gap increases the capacitance

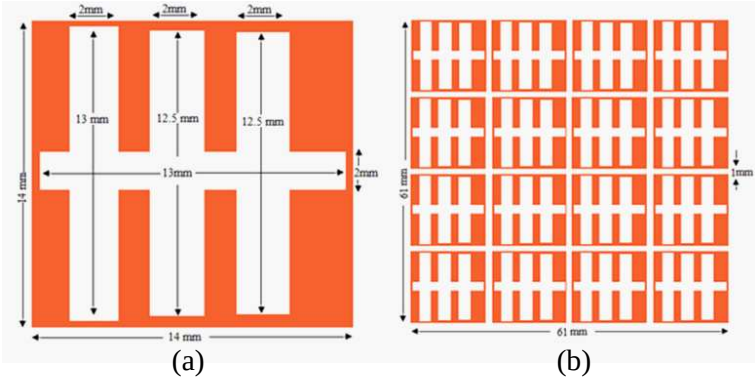

Figure 13. Proposed FSS structure. (a) Unit cell. (b) 4×4 FSS screen.

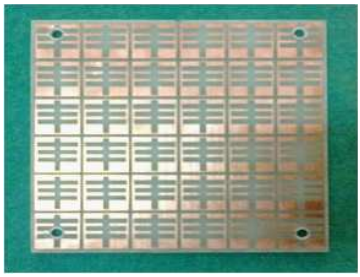

Figure 14. Photograph of the proposed FSS screen.

and as a result the resonant frequency shifts to the lower side. However the magnitude of the transmission characteristic remains almost same at -40 dB for all values of the spacing.

5.3. Effect of FSS on Antenna Characteristics

When the FSS is used as a superstrate layer, there is coupling between the patch and the FSS layer that affects the characteristics of antenna such as return loss, directivity and the gain. The coupling between the patch and the FSS is due to the fact that when waves radiated by antenna impinge on the FSS layer, the FSS layer reflects the waves in certain frequency bands. The reflected waves from FSS fall back on the patch antenna and affect the current distribution on the patch. This in turn affects the characteristics of the antenna. The coupling between the patch and the FSS depends upon the distance between the patch and the FSS superstrate. The Figure 17 shows the effect of height

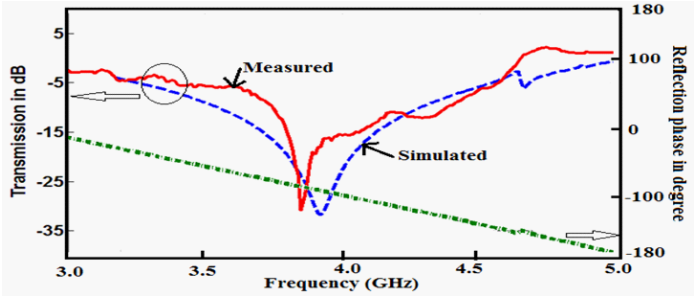

Figure 15. Measured and simulated transmission coefficient (dB) and reflection phase (in degrees) of the proposed FSS screen.

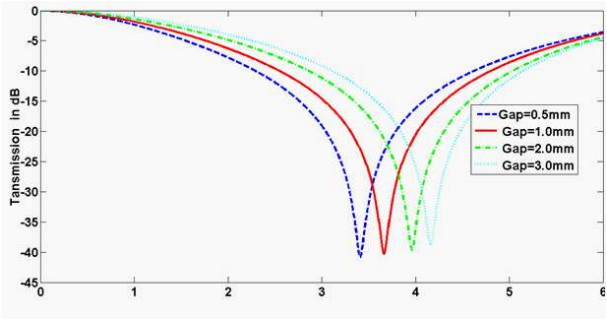

Figure 16. Effect of varying the unit cell spacing on the resonance frequency of the proposed FSS.

of FSS on the return loss and gain for the hexagonal patch antenna with slotted ground. As the FSS is used as a cover to the antenna, the electromagnetic waves which are radiated by the antenna illuminate the FSS which forces the distribution of electromagnetic waves in space and controls the phase. When the waves illuminate the FSS, the patches of FSS get excited and they work as aperture antennas. Also the transmission of waves from the the resonator to free space is angle dependent; for normal incidence there is 100% transmission and for incident angle other than normal angle there is attenuation of waves, i.e., the transmission is decided by the angle of incidence [19, 20].

The height of FSS is decided by the reflection phase and it is given by the following equation

$$\Psi_u + \Psi_l - 2\beta h = 2n\pi, \quad n = \ldots -2, -1, 0, 1, 2 \ldots \tag{4}$$

where Ψ_u and Ψ_l are the reflection phases of the upper reflector (FSS Screen) and the lower reflector (Ground) respectively, β is the

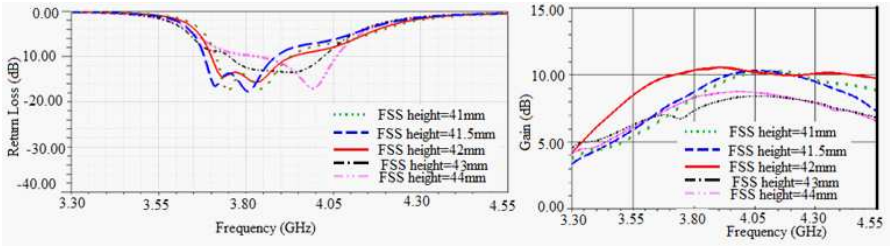

(a) (b)

Figure 17. Effect of the height of the aperture type FSS on (a) simulated return loss and (b) simulated peak gain for the antenna with slotted ground.

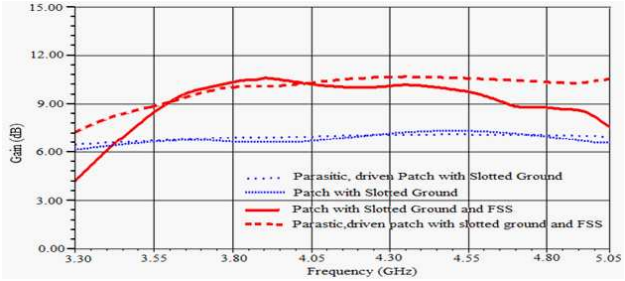

Figure 18. Effect of aperture FSS on the gain of hexagonal patch with slotted ground and on the antenna with parasitic element.

propagation constant equal to $2\pi/\lambda$ and h is the height of the FSS screen. In the case, the lower reflector is a ground plane, Ψ_l is equal to π and the height of the FSS will be primarily decided by the reflection phase of the FSS layer. It follows then that the optimal height of FSS for the aperture type FSS is approximately equal to $\lambda/2$; λ being the free space wavelength at the center frequency. This comes out to be 42 mm for the designed aperture FSS. The variation of gain for the hexagonal patch with slotted ground and for the antenna with parasitic element with and without the Aperture FSS screen is shown in Figure 18. The improvement in the gain due to the FSS screen is clearly visible with an increase of about 3 dB throughout the band.

For the proposed FSS, the reflection phase at 3.9 GHz is $-100°$ (as seen from Figure 15), and then, by Equation (4), the optimal height of FSS corresponding to $n = 0$ is calculated as 8.54 mm ($\lambda/9$), which is very less when compared to the aperture type of FSS for which it is 42 mm ($\lambda/2$). This shows the low profile nature of the proposed FSS over the aperture type FSS.

Since the FSS affects the current distribution on the patch, the

radiation undergoes a slight phase change. The amount of change in phase depends on the height of the FSS and can be optimized to change the direction of circular polarization. Hence, an optimal height can be found for the FSS so that the direction of circular polarization is changed to bore sight. The Table 4 shows the effect of FSS on the direction of circular polarization.

Table 4. Effect of aperture FSS on the simulated axial ratio and the direction of circular polarization.

Design	Lower 3 dB Axial ratio frequency (GHz)		Upper 3 dB Axial ratio frequency (GHz)	
	CST	HFSS	CST	HFSS
Hexagonal Patch with slot in the ground	3.8133	3.78	3.92	3.867
Hexagonal Patch with slot in the ground and with Aperture FSS	3.75	3.79	3.81	3.84
Antenna with parasitic element	3.50	3.55	3.56	3.6
Antenna with parasitic element and with Aperture FSS	3.5084	3.51	3.5778	3.55
Design	3 dB Axial Ratio Bandwidth (MHz)		Direction of circular polarization	
	CST	HFSS		
Hexagonal Patch with slot in the ground	106	87	$\theta = 240^\circ$ $\varphi = 210^\circ$	
Hexagonal Patch with slot in the ground and with Aperture FSS	60	50	$\theta = 0^\circ$ $\varphi = 0^\circ$	
Antenna with parasitic element	60	50	$\theta = 50^\circ$ $\varphi = 340^\circ$	
Antenna with parasitic element and with Aperture FSS	69	40	$\theta = 0^\circ$ $\varphi = 0^\circ$	

6. EXPERIMENTAL RESULTS WITH THE APERTURE TYPE FSS AND THE PROPOSED FSS

The return loss of the two antennas, i.e., the hexagonal patch with slotted ground and antenna with parasitic patch after application of FSS Screen (Aperture type the Proposed FSS) has been simulated and shown in Figures 19(a) and (b) respectively. It can be seen from the figure, that the return loss in case of the hexagonal patch with slot in the ground is nearly same in both the cases. The measured return loss without the FSS and with the application of the Aperture FSS and Proposed FSS are shown in Figures 20 and 21. Figure 20 is for the hexagonal patch with slotted ground and Figure 21 is for the antenna with parasitic patch. It is observed from both the figures that the measured return loss shifts towards the lower frequency side. It is because the proposed screen exhibits a capacitive loading effect on the patch.

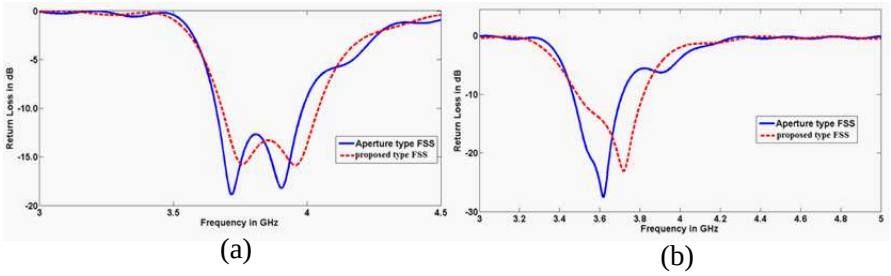

Figure 19. Simulated return loss after application of FSS of (a) HMP with slot in the ground, (b) HMP slotted ground with parasitic element.

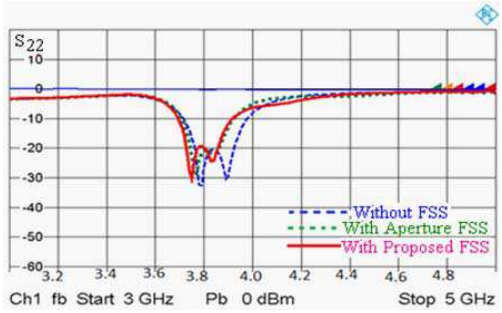

Figure 20. Measured return loss of the antenna with slotted ground with the aperture and proposed FSS.

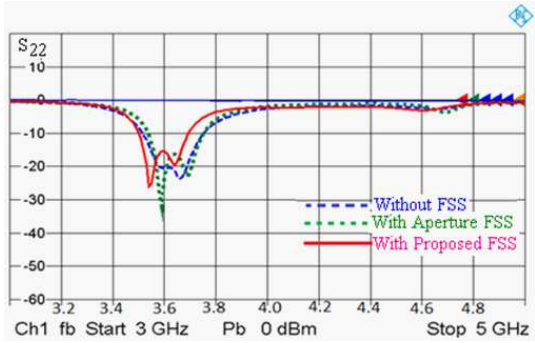

Figure 21. Measured return loss of the antenna with parasitic slot with the aperture and proposed FSS.

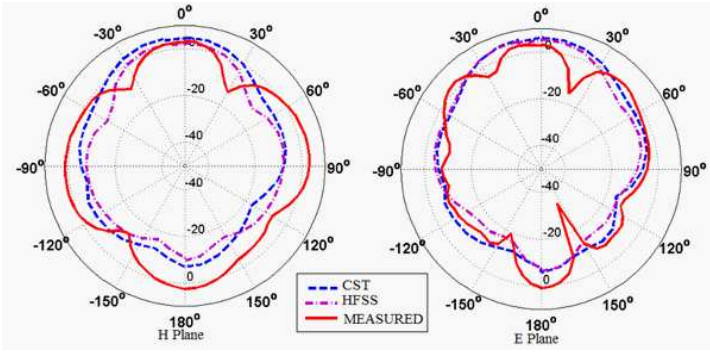

Figure 22. Measured and simulated radiation patterns of hexagonal patch with slot in the ground with proposed FSS ($h = 42$ mm)

6.1. Radiation Patterns and Peak Gain

The proposed FSS screen was applied to the antenna with the slotted ground and simulated for radiation patterns in the E and H-planes at the center frequency of the antenna. The FSS Screen was tested at both the heights, i.e., $\lambda/2$ (42 mm) and $\lambda/9$ (8.5 mm). The radiation patterns were also measured in the anechoic chamber. The measured and simulated patterns in both the planes for $h = 42$ mm are shown in Figure 22 whereas for $h = 8.5$ mm are shown in Figure 23. Similarly, radiation patterns of the antenna with parasitic element (simulated and measured) are shown in Figure 24 for $h = 42$ mm and in Figure 25 for $h = 8.5$ mm. The measured radiation patterns and the simulated ones are found to be in good agreement. A slight difference is observed between the radiation patterns for $h = 42$ mm and for $h = 8.5$ mm and this may be due to the increased cross polarization at $h = 8.5$ mm.

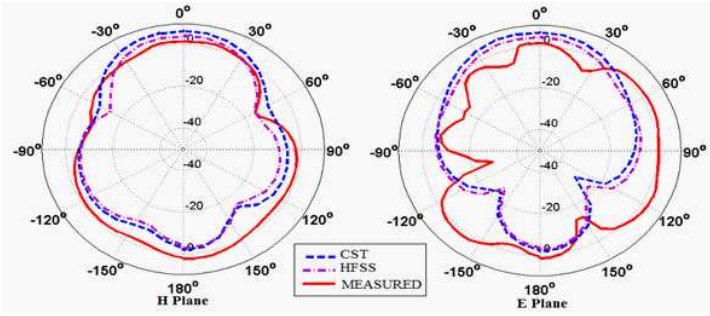

Figure 23. Measured and simulated radiation patterns of hexagonal patch with slot in the ground with proposed FSS ($h = 8.5\,\text{mm}$).

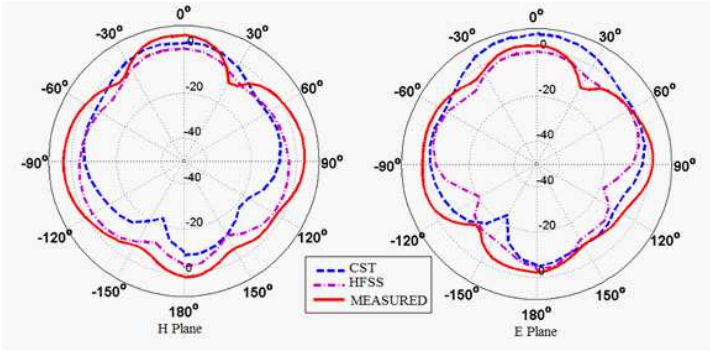

Figure 24. Measured and simulated radiation patterns of antenna with parasitic element with proposed FSS ($h = 42\,\text{mm}$).

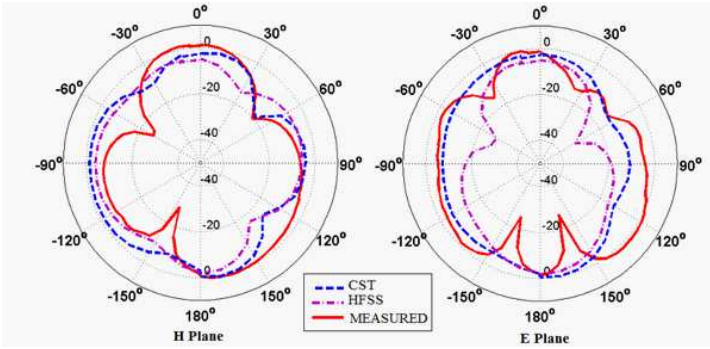

Figure 25. Measured and simulated radiation patterns of antenna with parasitic element with proposed FSS ($h = 8.5\,\text{mm}$).

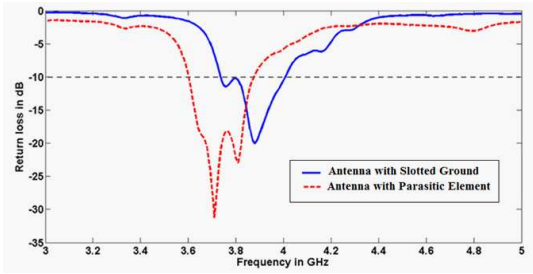

Figure 26. Measured return loss of HMP with slot in the ground and HMP with parasitic element after application of proposed FSS (with $h = 8.5\,\text{mm}$).

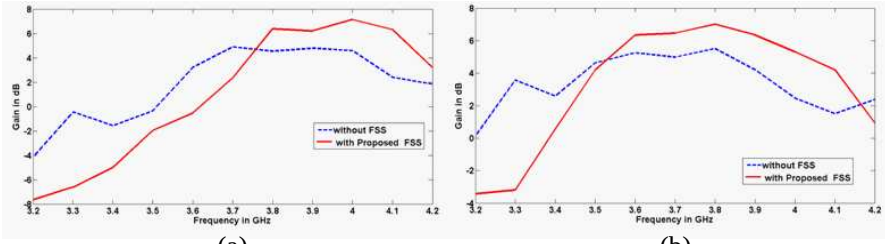

Figure 27. (a) Measured gain of the HMP with slot in the ground (without and with the proposed FSS at height $h = 8.5\,\text{mm}$). (b) Measured gain of the HMP with parasitic element (without and with the proposed FSS at height $h = 8.5\,\text{mm}$).

6.2. Return Loss and Gain with the Proposed FSS

Figure 26 shows the measured return loss of the HMP with slot in the ground and the HMP with parasitic element after application of Proposed FSS. The FSS was placed at height $h = 8.5\,\text{mm}$. The measured gain with and without the proposed FSS screen for the patch with the slotted ground is shown in Figure 27(a) while Figure 27(b) shows the measured gain for the antenna with parasitic element. An enhancement of gain by using the proposed screen is clearly evident.

7. CONCLUSION

A simple hexagonal patch, hexagonal patch with slot in the ground and antenna with parasitic element have been designed, fabricated and experimentally validated. The measured axial ratio for the HMP with

slotted ground and HMP with parasitic element is 4.73% and 3.33% respectively. The measured radiation patterns in the E and H planes are in good agreement with the simulated patterns. A compact FSS is proposed to enhance the gain which offers a size reduction of 25% over the conventional aperture type FSS. Using superstrate designed with this FSS, an improvement in the measured gain of around 3 dB for the HMP with slotted ground and 2 dB for the HMP with parasitic element is reported. Also a change in the direction of circular polarization towards the bore sight has been achieved by applying the proposed FSS. The antennas along with the FSS are very simple to design, low profile and useful for high gain applications in wireless communications.

ACKNOWLEDGMENT

The authors would like to thank the reviewers for their useful comments and suggestions. The first author likes to acknowledge the Vice Chancellor DIAT (DU), for financial support. Author also likes to acknowledge R. V. S. Rama Krishna for his technical suggestions.

REFERENCES

1. Pozar, D. M. and S. M. Duffy, "A dual-band circularly polarized aperture-coupled stacked microstrip antenna for global positioning satellite," *IEEE Transactions on Antennas and Propagation*, Vol. 45, No. 11, 1618–1625, Nov. 1997.
2. Sharma, P. and K. C. Gupta, "Analysis and optimized design of single feed circularly polarized microstrip antennas," *IEEE Transactions on Antennas and Propagation*, Vol. 31, No. 6, 949–955, Nov. 1983.
3. Garg, R., P. Bhartia, I. J. Bahl, and A. Ittipiboon, Editors, *Microstrip Antenna Design Handbook*, Artech House, 2001.
4. Ray, K. P., D. M. Suple, and N. Kant, "Suspended hexagonal microstrip antennas for circular polarization," *International Journal of Microwave and Optical Technology*, Vol. 5, No. 3, May 2010.
5. Ramirez, R. R., F. De Flaviis, and N. G. Alexopoules, "Single-feed circularly polarized microstrip ring antenna and arrays," *IEEE Transactions on Antennas and Propagation*, Vol. 48, No. 7, 1040–1047, Jul. 2000.
6. Bahl, I. J. and P. Bhartia, *Microstrip Antennas*, Artech House, Dedham, MA, 1980.

7. Kumar, G. and K. P. Ray, *Broadband Microstrip Antennas*, Artech House Publishers, London, 2003.
8. Pirhadi, A., H. Bahrami, and J. Nasri, "Wideband high directive aperture coupled microstrip antenna design by using a FSS superstrate layer," *IEEE Transactions on Antennas and Propagation*, Vol. 60, No. 4, 2101–2106, Apr. 2012.
9. Chen, H.-Y. and Y. Tao, "Bandwidth enhancement of a U-slot patch antenna using dual-band frequency-selective surface with double rectangular ring elements," *Microwave Opt. Technol. Lett.*, Vol. 53, No. 7, 1547–1553, Jul. 2011.
10. Monavar, F. M. and N. Komjani, "Bandwidth enhancement of microstrip patch antenna using Jerusalem cross-shaped frequency selective surfaces by invasive weed optimization approach," *Progress In Electromagnetics Research*, Vol. 121, 103–120, 2011.
11. Chaimool, S., K. L. Chung, and P. Akkaraekthalin, "Simultaneous gain and bandwidths enhancement of a single-feed circularly polarized microstrip patch antenna using a meta material reflective surface," *Progress In Electromagnetics Research B*, Vol. 22, 23–37, 2010.
12. Arnaud, E., R. Chantalat, M. Koubeissi, T. Monediere, E. Rodes, and M. Thevenot, "Global design of an EBG antenna and meander-line polarizer for circular polarization," *IEEE Antennas and Wireless Propagation Letters*, Vol. 9, 215–218, 2010.
13. Arnaud, E., R. Chantalat, T. Monediere, E. Rodes, and M. Thevenot, "Performance enhancement of self-polarizing metallic EBG antennas," *IEEE Antennas and Wireless Propagation Letters*, Vol. 9, 538–541, 2010.
14. Singh, D., A. Kumar, S. Meena, and V. Agarwala, "Analysis of frequency selective surfaces for radar absorbing materials," *Progress In Electromagnetics Research B*, Vol. 38, 297–314, 2012.
15. Lin, H.-N., K.-W. Lin, and S.-C. Chen, "Use of frequency selective surfaces to prevent SAR and improve antenna performance of cellular phones," *PIERS Proceedings*, 214–218, Suzhou, China, Sep. 12–16, 2011.
16. Munk, A., *Frequency Selective Surfaces: Theory and Design*, Wiley-Interscience, New York, 2000.
17. Da Silva, M. R., C. de L. N_obrega, P. H. da F. Silva, and A. G. D'Assuncao, "Dual-polarized band-stop fss spatial filters using vicsek fractal geometry," *Microwave Opt. Technol. Lett.*, Vol. 55, No. 1, Jan. 2013.
18. Agrawal, P. and M. C. Bailey, "An analysis technique for

microstrip antennas," *IEEE Transactions on Antennas and Propagation*, Vol. 25, No. 6, 756–759, Nov. 1977.

19. Thèvenot, M., M. S. Denis, A. Reineix, and B. Jecko, "Design of a new photonic cover to increase antenna directivity," *Microwave Opt. Technol. Lett.*, Vol. 22, No. 2, 136–139, Jul. 1999.
20. Weily, A. R., K. P. Esselle, T. S. Bird, and B. C. Sanders, "High-gain 1D EBG resonator antenna," *Microwave Opt. Technol. Lett.*, Vol. 47, No. 2, 107–114, 2005.